VOL. 12, NO. 4, FEBRUARY 2017 ISSN 1819-6608
ARPN Journal of Engineering and Applied Sciences

www.arpnjournals.com

0.1-10 THz SINGLE PORT LOG PERIODIC ANTENNA DESIGN BASED ON HILBERT GRAPHENE ARTIFICIAL MAGNETIC CONDUCTOR

Hussein A. Abdulnabi[1], Refat T. Hussein[2] and Raad S. Fyath[3]
[1]Department of Electrical Engineering, University of Technology, Iraq
[2]Depatment of Communication Engineering, University of Technology, Baghdad, Iraq
[3]Department of Computer Engineering, AL-Nahrain University, Iraq
E-Mail: Hussein_ali682@yahoo.com

ABSTRACT

In this work, a single port toothed log periodic antenna (TLPA) based on Hilbert curvegraphene artificial magnetic conductor (AMC) is proposed for frequency band (0.1–10) THz operation. The bandwidth and resonance frequency of the proposed antenna can be tuned by changing the connected DC voltage which leads tovariation in the chemical potential of graphene. The radiating element of the TLPA isgold patch placed on Hilbert curve graphene AMC. Exponential taper is used to satisfy impedance matching between the antenna and the feeder over the required frequency range. The simulation results reveal that 100 % of the frequency range satisfies $s_{11} < -10\ dB$ when chemical potential is1eV.

Keywords: graphene, artificial magnetic conductor, terahertz antenna, toothed log periodic antenna, UWB antenna, hilbert curve.

1. INTRODUCTION

The crowded wireless communication bands in the gigahertz (GHz) frequency range and the ever-increasing demand for more bandwidth has motivated the exploitation of the unexplored spectrum of electromagnetic waves such as the terahertz (THz) band. The higher bandwidth of the THz band has a potential to achieve an extremely high data rate, such as 1 terabit-per-second, for future wireless devices [1]. The THz band corresponds to the segment of the electromagnetic spectrum from (0.1–10) THz (i.e., wavelengths in the range of 3 mm ~ 0.3 mm) in between the millimeter and far-infrared (IR) waves [2]. As terahertz technology has attained maturity. THz spectroscopy, imaging, and other various applications have grown considerably in the last decade.

Metals, in particular, gold, are commonly used to fabricate antennas in the THz frequency range. At THz frequencies, the lower conductivity of metal, compared to its DC conductivity, increases field penetration into the metal. This behavior of metal at THz frequencies degrades the radiation efficiency of metallic antennas [4]. A numerical analysis showed that small-scaled antennas have much lower radiation efficiency at 1 THz due to the high surface resistance of metallic traces [5]. Also, as a result of the fabrication and method of gold deposition needed for achieving thin layers with a small trace width of less than 100 nm, the conductivity values of gold are considerably lower than that of the bulk material. This lower conductivity is due to grain boundary scattering, surface scattering, and surface roughness [6, 7]. These factors can considerably reduce the theoretically predicted radiation efficiency of antennas at THz band and higher. To control losses in small-scale antennas, materials other than metals should be considered. The latest new material in the quest of miniaturized THz devices is graphene.

Graphene has been named the simplest complex material which has drawn increasing attention in recent years due to its unique properties and advantages. In fact, graphene is used in many fields including mechanical, thermal and electrical applications [8]. The surface conductivity of the graphene can be tuned by changing the applied electrical potential [9], thus many graphene based-devices such as antennas, filters, absorbers, and polarizer's have been suggested for bands in microwave, terahertz and optical frequencies [10]. Graphene-based THz and photonic antennas were also developed in [11].

The graphene can be used to design THz antennas, as radiating part [12], parasitic component, or high impedance surfaces (HIS) usually based on AMC configuration [13]. AMC is a planar array of periodic surface which can improve the control of electromagnetic wave radiation. Thus this structure has been broadly utilized in the design of some types of antennas such as low profile leaky-wave antenna operating at microwave regime with high efficiency and gain in correlation with conventional ground plane. Also adding active HIS [14] elements loaded with varactor diodes to the antennas enables them to beam steering and easy frequency tuning [15]. It is possible to insert periodic graphene patches as antenna ground. A tunable terahertz antenna based on graphene AMC with relatively narrow bandwidth was presented in [16]. In [17] many shapes of grapheme-based AMC were studied and compared. The graphene biased reflective array was also applied for the antenna to get frequency tuning and beam reconfiguration [12].

In this work, a novel tunable UWB antenna depends on Hilbert curve AMC array is proposed. The antenna is a log periodic toothed shape with exponential tapered transmission line implemented over graphene patches array which acts as AMC. The applied voltage is used to tune this antenna in order to wide its bandwidth.

2. BACKGROUND

2.1 Graphene conductivity

The graphene can displayed as an infinitesimally flimsy surface which is portrayed by surface

conductivity $\sigma(\omega, \tau, \mu_C, T)$. The graphene conductivity Drude model can be written by [18]

$$\sigma\left(\omega, \mu_c, \gamma, T\right) = \frac{je^2(\omega - j2\gamma)}{\pi\hbar^2}\left[\frac{1}{(\omega - j2\gamma)^2}\int_0^\infty \epsilon\left(\frac{\partial f_d(\epsilon)}{\partial \epsilon} - \frac{\partial f_d(-\epsilon)}{\partial \epsilon}\right)d\epsilon - \int_0^\infty \epsilon\left(\frac{\partial f_d(-\epsilon) - f_d(\epsilon)}{(\omega - j\,2\gamma)^2 - 4(\epsilon/\hbar)^2}\right)d\epsilon\right] \quad (1)$$

In the above equation, $f_d = (e^{(\epsilon-\mu_c)/k_B T} + 1)^{-1}$ is the Fermi-Dirac distribution?

ω = Angular frequency in rad / second and

γ =Scattering rate in s^{-1}

μ_c = Chemical potential in eV, which can be controlled by chemical doping or by applying a bias voltage

T = Temperature in Kelvin

e = Electron charge

ħ = Reduced Planck's constant, and

k_B =Boltzmann constant

The first term in Eq. (2) is due to the intraband contribution, and the second term is from the inter-band contribution. The Kubo formula is in an integral form which makes it hard to evaluate as well as to integrate with the finite difference time domain FDTD scheme. The Kubo formula can be simplified [21], and the intra-band conductivity is:

$$\sigma = \sigma_{intra} + \sigma_{inter} \quad (2)$$

$$\sigma_{intra}(\omega, \mu_c, \gamma, T) = \frac{e^2 k_B T \tau}{\pi\hbar^2}\left[\frac{\mu c}{k_B T} + 2\ln\left(e^{\frac{-\mu_c}{k_B T}} + 1\right)\right]\frac{1}{\omega - j2\gamma} \quad (3)$$

The intraband term dominates the graphene conductivity over an ultrawide band of frequencies, from DC up to 1 THz, the real part of the intra band conductivity being much larger than the imaginary part in this frequency range [21]. The interband conductivity can be expressed as

$$\sigma_{inter}(\omega, \mu_c, \gamma, T) = \frac{-je^2}{4\pi h}\ln\left(\frac{2|\mu_c| - (\omega - j2\gamma)h}{2|\mu_c| + (\omega - j2\gamma)h}\right) \quad (4)$$

The interband conductivity dominating above 1 THz, its real part being much smaller than its imaginary part. Although the interband conductivity is much larger than the intraband conductivity in the THz range, both terms were taken into account for the calculation of the surface impedance.

Graphene surface impedance can be obtained from its conductivity by using the equation

$$Z_S = 1/\sigma(\omega) = R_S(V_b) + j\,X_S(V_b) \quad (5)$$

2.2 Hilbert curve AMC

There are many types of fractal shapes that have been proposed after it was coined out by Mandelbrot in1975.The Hilbert curve has been proposed by Hilbert in 1981. The geometries were generated initerative patterns. Hilbert curve shape is categorized as the space filling curves group. The curves employed allow further reduction in the antenna size, thus allow compacting of the antenna size while maintaining the performance [8, 9].

Figure-1 shows the Hilbert curve antenna (HCA) configurations. Here D, d and b are the antenna width, fractal segment or spacing and antenna linewidth, respectively. For the first iteration, the AMC length and fractal segment are of the same dimensions. For the second and successive iterations, the fractal segment or spacing can be computed with proper.

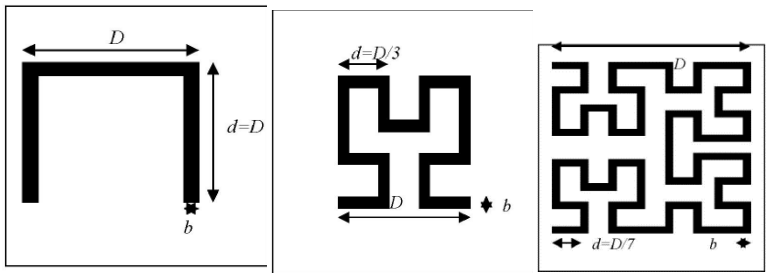

(a) First iteration (b) Second iteration c) Third iteration

Figure-1. Hilbert curve AMC [12].

The mathematical approach for designing the antenna is based on the resonant meander line [12].For an HCA with outer dimension l and order of fractal iteration n, the length of each line segment d is given by the formulation:

$$d = \frac{l}{2^n - 1} \quad (6)$$

In an HCA geometry of order n, there arem short-circuited parallel wire sections lengths d is given

m=4^{n-1}

The sum of all the line segments (s) is

$$s = (2^{2n} - 1)d \quad (7)$$

2.3 Log periodic antenna

Log periodic antenna (LPA) is still interesting although many decades passed. It provides frequency independence properties for the antenna over wide band of frequency. In fact theoretically log periodic antenna is a class of antennas for which pattern and impedance independent on frequency for unlimited band of frequencies. The impedance and pattern of LPA structures

is shaped so that repeat periodically in relation with the frequency logarithm, as in Figure-2.

$$\tau = \frac{R_{N+1}}{R_N} \quad (8)$$

$$\sigma = \frac{r_N}{R_N} \quad (9)$$

where $R_N$and r_N are the distance from the center of the antenna to the outer and inner radiuses of the tooth N respectively, τ is the ratio between two outer radiuses of successive teeth and σ is the ratio between inner radius to the outer radius for any tooth. The structure shape and scaling factor τ can be used such that the changing of the impedance and pattern over each period is small, the result being an extremely wideband antenna. The feeding of the two parts of the antenna is at the vertices either by a coaxial line or by a balanced two-wire line. The upper and lower frequency limits are achieved when the shortest and longest teeth respectively, are around0.25 wavelength long.

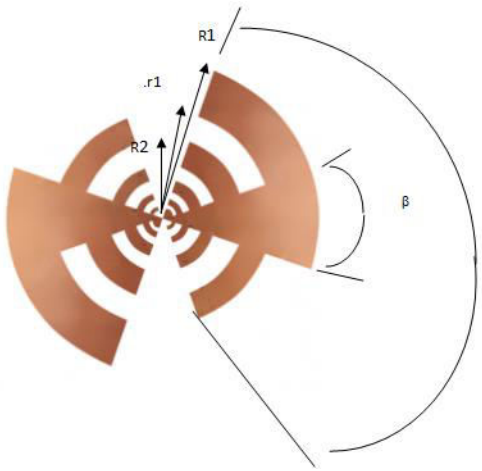

Figure-2. Log periodic toothed antenna.

2.4 Impedance matching

Tapered line is used in this work to increase the matching between the antenna and the feeder. Typically the characteristic impedance of the transmission line is 50Ω, while the input impedance of the proposed wideband antenna is 200Ω. Thus an exponential line taper is used to match the 50Ω of the feeder to the 200Ωof the antenna, as shown in Figure-3. The exponential line is characterized by [20]

$$Z(z) = Z_o e^{az} \; for \quad 0 \le z \le L$$

$$where \;\; Z_o = Z(0) \text{ and}$$

$$a = \frac{1}{L} ln(\frac{Z_L}{Z_O}) \quad (10)$$

Here $Z(L)$ is the characteristic impedance of the transmission line at distance L, then $Z_L \equiv Z(L)$.

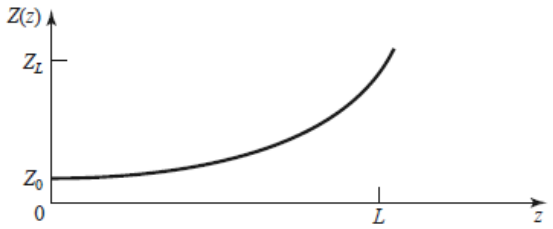

Figure-3. Variation of the characteristic impedance along the exponential taper.

3. PROPOSED ANTENNA AND SIMULATION RESULTS MODEL

The proposed antenna consists of LPTA radiating element made from gold material is based on grapheme Hilbert curve AMC array instead of square patchas shown in Figure 4b. A groundedSiO_2material of thickness10 μm is representing the AMC substrate. A silicon wafer of thickness 300 μm is used under the substrate. A50 nm from polycrystalline silicon material is placed above the quartz is thick layer and Al_2O_3 of 10 nm-thick film in sequence [16].The AMC unit consists of Hilbert curve array based on graphene. A 2 μm-thick SiO_2 materialis placed on graphene-based AMC, andthe gold antenna placed on Sio_2layer. As in our previous work [19] The LPTA has a structure of $\alpha = 120^0 \; and \; \beta = 45^{o,}$ where α is the tooth angle, β is the bowtie angle, $\tau = \sigma^2 = 0.5$, and $L = 220 \; \mu m$.

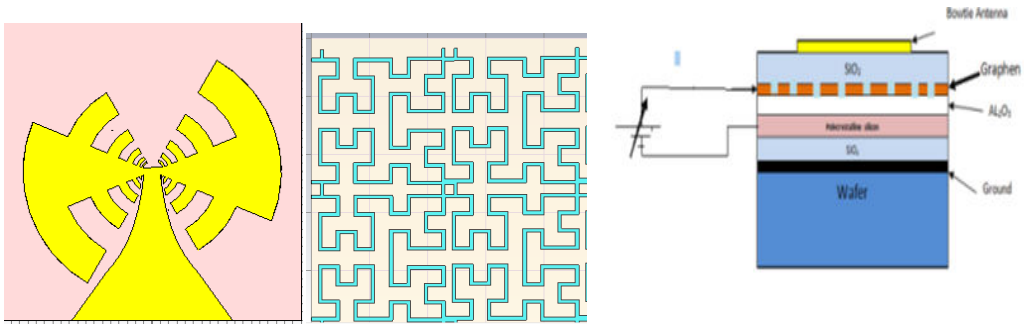

(a) Log periodic antenna (b) graphene AMC (c) side view

Figure-4. Proposed log periodic antenna and Hilbert curve graphene AMC.

Simulation results related to the proposed antenna are obtained using CST Studio ver.2014 for many values of chemical potential μ_C.Results related to $\mu_C = 0.2eV\ to\ 1eV$ aregiven.

Figure-5a shows the scattering parameter S_{11} in dB of the proposed antenna for $\mu_C = 0.2eV$. The operating bandwidth extends from (1.2 – 3.5), (4-5.6) and (7.3 – 10) THz, at which S_{11}< -10 dB, while Figure 5b shows the antenna has gain ≥ 0 dB for the frequency band (0.1 - 5.5) THz.

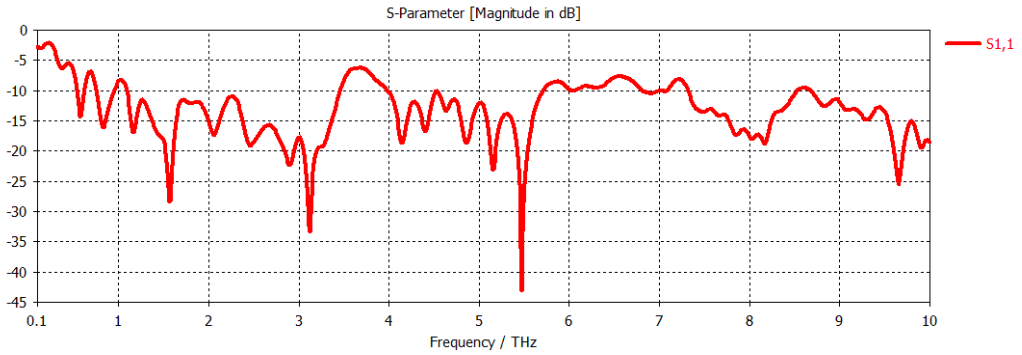

(a) Scattering parameter S_{11}

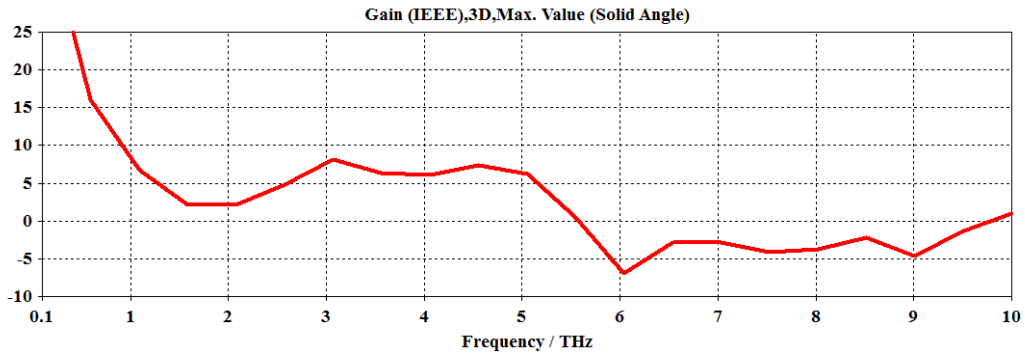

(b) Antenna gain

Figure-5. Antenna characteristics when $\mu_C = 0.2eV$.

Figure6a shows the scattering parameter S_{11} in dB of the antenna for $\mu_C = 0.4eV$. The operating bandwidth extends from (0.8 -6.6), (8.5 – 10) THz also there are resonance frequency at0.5 THz at which $S11 < -10\ dB$.

Figure-6b shows the broadband gain of the proposed antenna for $\mu_C = 0.4eV$. It has gain≥ 0 dB for the frequency band (0.1-8) THz.

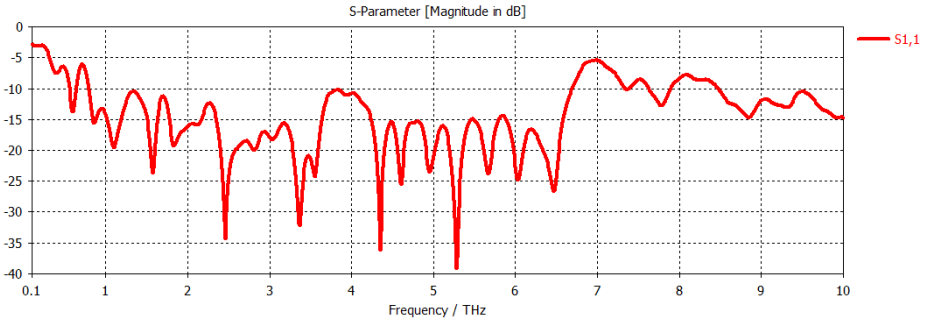

(a) Scattering parameter S_{11}

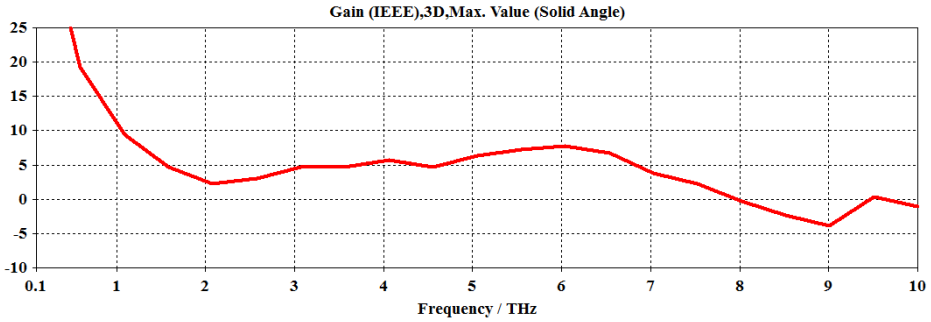

(b) Antenna gain

Figure-6. Antenna characteristics when $\mu_C = 0.4eV$.

Figure7a shows the scattering parameter S_{11} in dB of the proposed antenna for $\mu_C = 0.6\ eV$.The operating bandwidth extends from (0.8 -1.8), (2-7.2) and (8-10) THz also there are resonance frequency at 0.5 THz at which $S11 < -10\ dB$.

Figure-7b shows the broadband gain of the proposed antenna for $\mu_C = 0.6eV$. It has good gain ≥ 1 dB for the frequency band (0.1-10)THz.

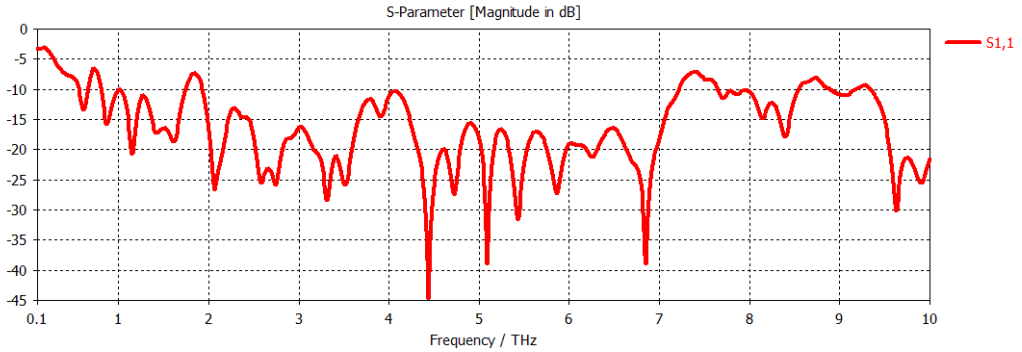

(a)Antenna scattering parameter S_{11}

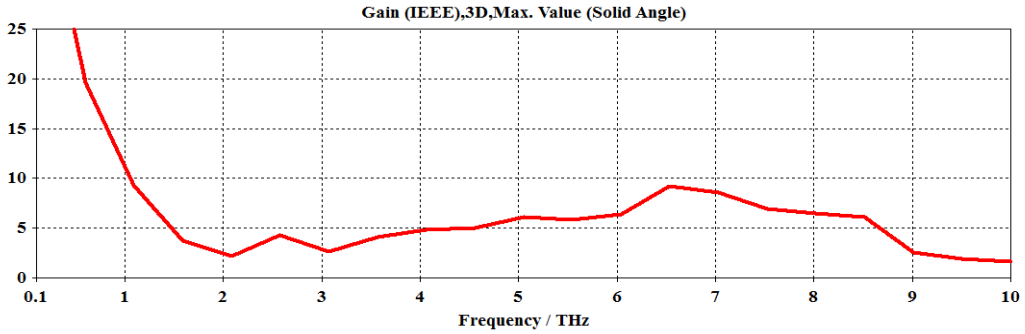

(b)Antenna gain

Figure-7. Antenna properties when μ_c=0.6 eV.

Figure-8a shows the scattering parameter S_{11} in dB of the proposed antenna for $\mu_C = 0.8eV$.The operating bandwidth extends from (0.8 -10) THz atwhich $S11< -10\ dB$.

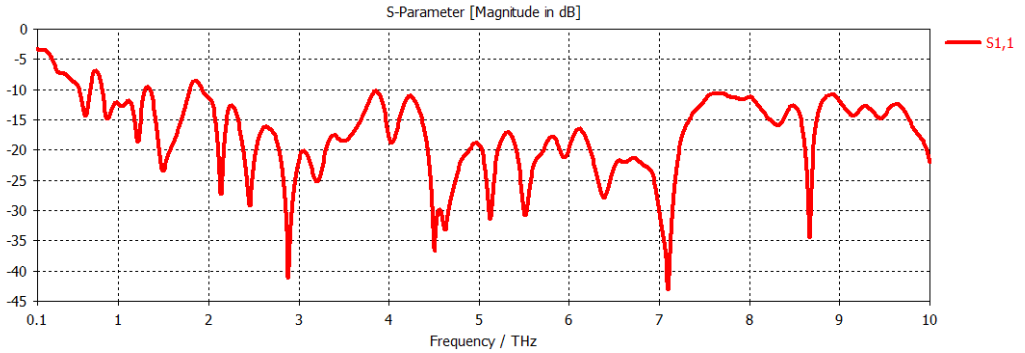

(a) Antenna scattering parameter S_{11}

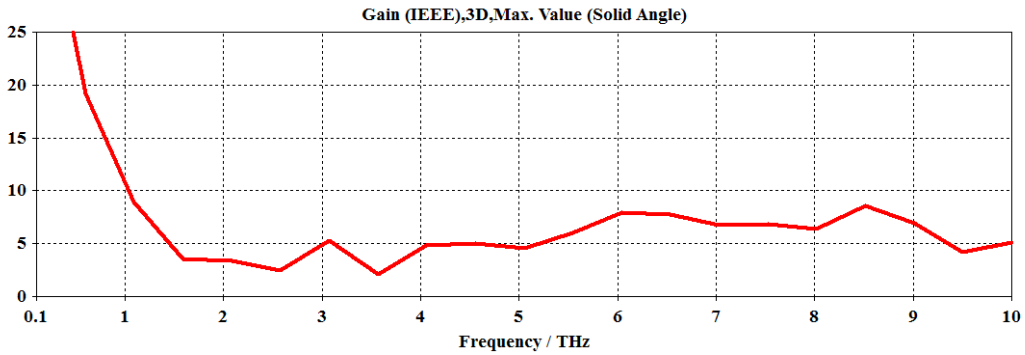

(b) Antenna gain

Figure-8. Antenna scattering parameter S_{11} when μ_c=0.8 eV.

Figure-9a shows the scattering parameter S_{11} in dB of the proposed antenna for $\mu_C = 1eV$. The operating bandwidth extends from (0.5 -10) THz at which $S11< -10\ dB$.

Figure-9b shows the broadband gain of the proposed antenna for $\mu_C = 1eV$. It has good gain ≥ 2 dB for the frequency band (0.5-10) THz.

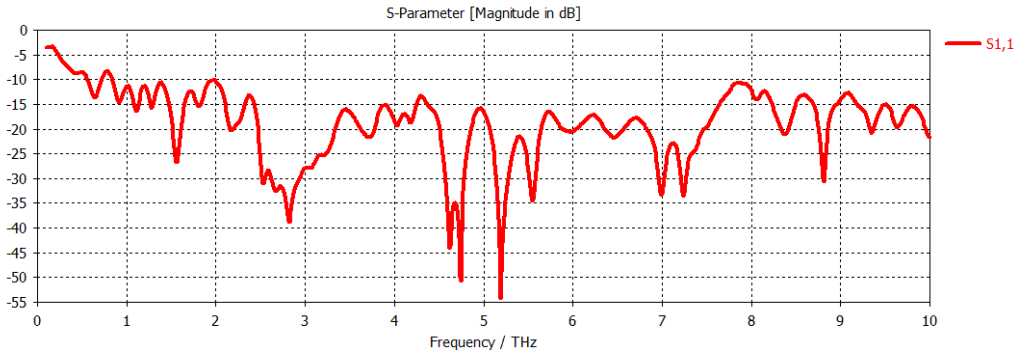

(a) Antenna scattering parameter S_{11}

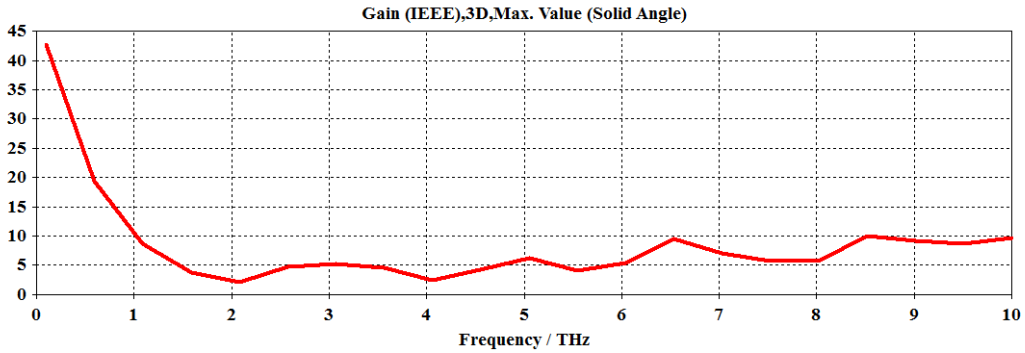

(b) Antenna gain

Figure-9. Antenna scattering parameter S_{11} when μ_c=1 eV.

4. CONCLUSIONS

In this work, a tunable antenna based on Hilbert curve graphene as artificial magnetic conductor has been designed to achieve UWB operating frequency band, (0.1 -10)THz at which S_{11}< -10 dB. The antenna itself has been formed as log periodic toothed antenna from gold material where an exponential transmission line taper is used to satisfy the matching between the antenna and the feeder. The simulation results have been obtained using CST Studio ver. 2014 by changing the values of the chemical potential $\mu_C = 0.2eV\ to\ 1eV$. The proposed antenna satisfies a highest bandwidth extends from (0.5 -10) THz at which $S11 < -10\ dB$ when $\mu_C = 1eV$. Also, it has good gain ≥ 2 dB for the frequency band (0.5-10) THz.

ACKNOWLEDGEMENT

One of the authors, Hussein Ali would like to thank the college of Engineering at AL- Mustansiriyah university, Baghdad, Iraq, http://uomustansiriyah.edu.iq/index.php?id_dept=5 for offering the PhD. Scholarship.

REFERENCES

[1] I. F. Akyildiz, J. M. Jornet, and C. Han. 2014. Terahertz band: Next frontier for wireless communications. Physical Commun. 12: 16-32.

[2] P. H. Siegel. 2002. Terahertz technology. IEEE Trans. Microwave Theory and Techniques. 50: 910-928.

[3] M. Walther, D. Cooke, C. Sherstan, M. Hajar, M. Freeman, and F. Hegmann. 2007. Terahertz conductivity of thin gold films at the metal-insulator percolation transition. Physical Rev. B. 76: 125408.

[4] G. Hanson. 2008. Radiation efficiency of nano-radius dipole antennas in the microwave and far-infrared regimes. IEEE, Trans. Antennas and Propag. Mag. 50: 66-77.

[5] N. Laman and D. Grischkowsky. 2008. Terahertz conductivity of thin metal films. Appl. Phys. Lett. 93: 051105.

[6] T. Kuan, C. Inoki, G. Oehrlein, K. Rose, Y. P. Zhao, G. C. Wang. 2000. Fabrication and Performance limits of sub-0.1 μm Cu Interconnects. in MRS Proceedings.

[7] A. K. Geim and K. S. Novoselov. 2007. The rise of grapheme. Nature Mat. 6(3): 183-191.

[8] B. Sensale - Rodr´ıguez, R. Yan, L. Liu, D. Jena and H. G. Xing. 2013. Graphene for reconfigurable terahertz optoelectronics. Proc. IEEE. 101(7): 1705-1716.

[9] A. Fallahi and J. Perruisseau-Carrier. 2012. Design of tunable bi-periodic graphene metasurfaces. Phys. Rev. B. 86(195408).

[10] B. Wu, H. M. Tuncer, M. Naeem, B. Yang, M. T. Cole, W. I. Milne, and Y. Hao. 2014. Experimental demonstration of a transparent graphene millimeter wave absorber with 28% fractional bandwidth at 140 GHz. Sci. Rep. 4130 4(4130).

[11] M. Esquius-Morote, J. S. G´omez-D´ıaz, and J. Perruisseau-Carrier. 2014. Sinusoidally modulated graphene leaky-wave antenna for electronic beam scattering at THz. IEEE Trans. Terahertz Sci. Technol. 4(1): 116-122.

[12] M. Dragoman, A. A. Muller, D. Dragoman, F. Coccetti and R. Plana. 2010. Terahertz antenna based on grapheme. J. Appl. Phys. 107(10): 104 313.

[13] Y. Huang, L. S.Wu, M. Tang and J.Mao. 2012. Design of a beam reconfigurable THz antenna with graphene-based switchable high-impedance surface. IEEE Trans. Nanotechnol. 11(4): 836-842.

[14] R. Guzman-Quiros, J. L. Gomez-Tornero, A. R. Weily and Y. J. Guo. 2012. Electronically steerable 1-D Fabry-Perot leaky-wave antenna employing a tunable high impedance surface. IEEE Trans. Antennas Propag. 60(11): 5046-5055.

[15] X. C. Wang, W. S. Zhao, J. Hu, and T. Zhang. 2013. A novel tunable antenna at THz frequencies using graphene-based artificial magnetic conductor (AMC). Prog. Electromagn. Res. Lett. 41: 29-0-38.

[16] X. C. Wang, W. -Y. Li, W.-S.Zhao, J. Hu. 2013. Comparative study on graphene - based artificial magnetic conductor (AMC). PIERS proceedings, Sweden. pp. 496-499.

[17] S. A. Amanatiadis, N. V. Kantartzis. 2013. Graphene-Based Patch Nano-Antennas with Optimal Width-Adjustable Radiation Characteristics. IEEE. Electromag. In Advan. Applic. (ICEAA), Inter. Conf.., Torino.

[18] Hussein A. Abdulnabi, Refat T. Hussein, and Raad S. Fyath. 2017. UWB single port log periodic toothed terahertz antenna design based on graphene artificial magnetic conductor. Modern Applied Science (accepted and the publishing date in Mar. 2017).

[19] D. M. Pozar. 2011. Microwave Engineering. 4th Ed., Wieley. p. 263.

[20] M. Dragoman M. Aldrigo A. Dinescu, D.Dragoman, and A. Costanzo. 2014. Towards a terahertz direct receiver based on graphene up to 10 THz. J. Appl. Phys. 115, 044307.